

**LUNAR PITS AND CAVES: THERMAL ENVIRONMENT AND VOLATILE-TRAPPING POTENTIAL.** A. X. Wilcoski<sup>1</sup>, P. O. Hayne<sup>1</sup>, and C. M. Elder<sup>2</sup> <sup>1</sup>University of Colorado, Boulder, CO, <sup>2</sup>Jet Propulsion Laboratory, California Institute of Technology (andrew.wilcoski@colorado.edu).

**Introduction:** Lunar pits are steep-walled, negative relief features that are interpreted to have formed by the collapse of the surface into a subsurface void, and may therefore be connected to other subsurface features such as overhangs, caves, and lava tubes (Fig. 1) [1]. These features are attractive targets for future human and robotic missions due to the insights they may give into lunar impact and volcanic processes, as well as the shelter from radiation and micrometeorites that they could provide to support a long-term human presence on the Moon.

At high latitudes ( $>70^\circ$ ) pit interiors tend to become Permanently Shadowed Regions (PSRs) due to their steep-walled nature. Lunar PSRs are of interest due to the potential for some PSRs to remain at temperatures cold enough to allow water ice and other volatiles to be stable over billion-year timescales [2]. This has led to the suggestion that high-latitude pits and caves could provide environments favorable to the accumulation of volatiles, while shielding them from processes that could destroy volatiles (e.g., micrometeorite bombardment) [3,4,5]. If concentrations of volatiles were found in high-latitude pits and caves, they could serve as a record of the history of volatiles on the Moon, as well as a potential resource during future human exploration.

Wagner and Robinson [1] identified 228 pits within  $50^\circ$  of the equator, mostly within impact melt deposits, and further studies [3,4] have identified pit candidates at higher latitudes. Though the high solar incidence angle at high latitudes makes distinguishing pits from other shadowed regions difficult, there is no reason to believe that impact melts at high latitudes would be less likely to host pits than those at low latitudes.

While latitude and shadowing strongly control a pit's interior temperature, its geometry can also have a large effect on both temperature and volatile trapping potential. For example, steep walls can increase shadowing relative to a crater, but may also increase multiple-scattering of radiation within a pit. Geometry may also make it harder for volatile molecules to ballistically escape from a pit.

In this study, we model the thermal environments within high-latitude pits and caves in order to answer two main questions: (1) How does pit/cave interior temperature vary with latitude and geometry? (2) How do pit temperature and geometry affect volatile stability for a range of different volatiles, including water?

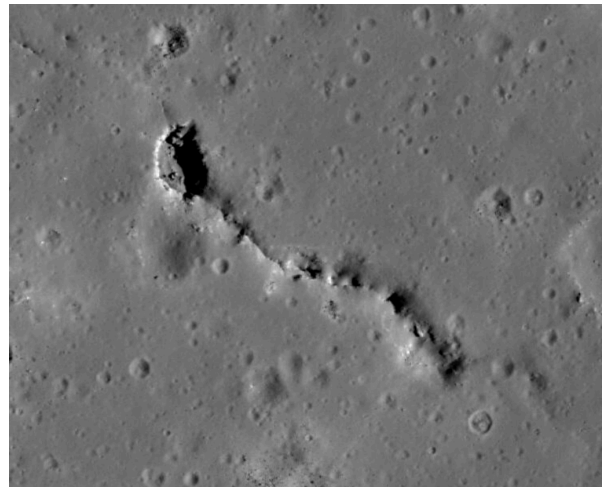


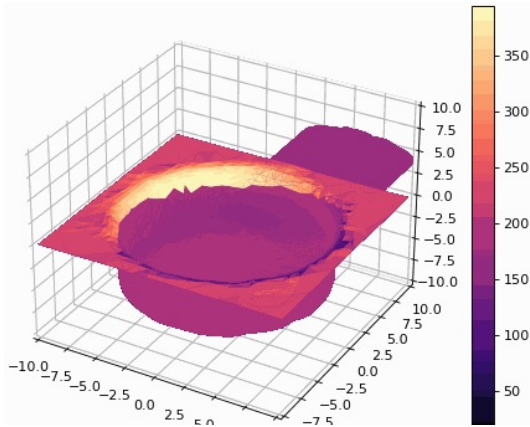
**Figure 1** Elliptical pit connected to a fracture/depression at  $6.36^\circ$  N,  $119.93^\circ$  E. LROC image M128509025RE (NASA/GSFC/ASU)

**Methods:** We create and validate a 3D thermal model to determine temperatures within lunar pits/caves of different geometries and latitudes. The model is initialized with a 3D surface composed of triangular facets. Surface temperatures on each facet are calculated by balancing direct insolation, 1D heat conduction perpendicular to the surface, infrared emission, and multiple-scattering of both visible and infrared radiation. The model also accounts for terrain shadowing on each facet.

We examine thermal environments within a number of different geometries chosen based on the pit observations made by [1]. Geometries of interest include cylindrical pits, pits connected to caves, and narrow fractures similar to those found in impact melts. For each geometry, we run the thermal model over a range of latitudes from the equator to pole. For the narrow fractures, we consider both north-south and east-west orientations. The thermal model outputs the temperature of each facet of the 3D surface over time.

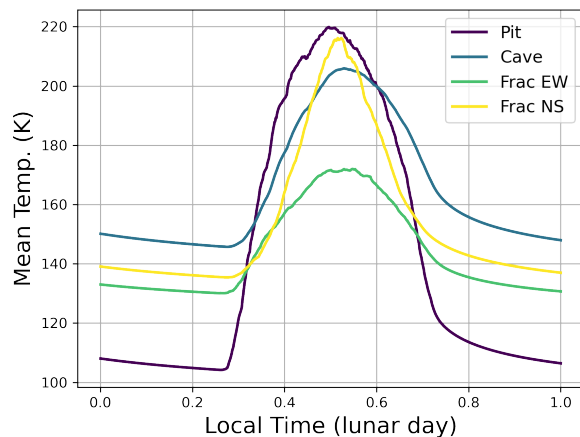
We also developed a volatile transport model that determines volatile mass balance within a pit based on the pit's interior temperatures. Volatile loss from each facet is modeled by analogy with a radiative process, where fluxes of particles between facets are treated in the same way as fluxes of radiation. Surface temperatures control these particles fluxes through their surface residence times. The volatile transport model allows us to assess the residence time of a species within a pit given some initial quantity of that species.

**Results:** Figure 2 shows modeled surface temperatures for a cylindrical pit with an attached cave at  $-80^\circ$  latitude shortly before local noon. The highest



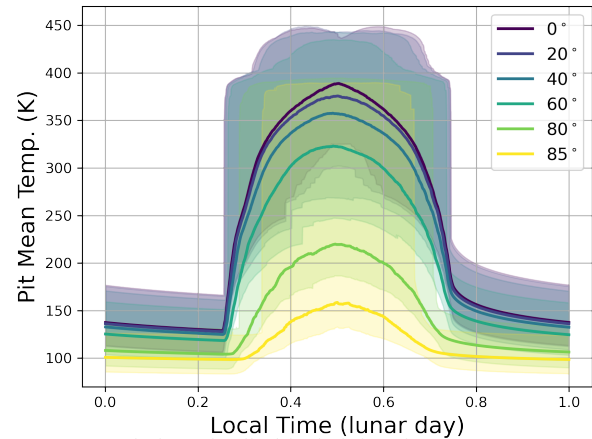
**Figure 2** Modeled surface temperatures of a cylindrical pit with attached cave. The colorbar units are degrees Kelvin. temperatures occur on the equator-facing pit rim, and most of the pit remains in shadow due to its high latitude. Reradiated infrared emission is the dominant energy source for shadowed facets.

Figure 3 shows the instantaneous mean temperature within a cylindrical pit at each timestep for pits at latitudes between  $0^\circ$  and  $85^\circ$ . The shaded areas around each curve are bounded by the maximum and minimum pit temperatures at each timestep. Pit mean temperature decreases as a function of increasing latitude, and decreases more rapidly at latitudes above  $\sim 60\text{--}70^\circ$  where pits begin to develop PSRs.



**Figure 4** Mean temperature vs time for a cylindrical pit (purple), an attached cave (blue), an east-west fracture (green), and a north-south fracture (yellow).

Figure 4 shows the instantaneous mean temperature versus time within pits of four different geometries. The East-West oriented fracture achieves the coldest daytime mean temperatures. The cave and E-W fracture maintain the most stable temperatures over a lunar day, due to zero or almost zero direct insolation combined with efficient infrared reradiation among facets within these features. The cylindrical pit achieves the highest mean temperatures due to a significant portion of the pit rim receiving direct insolation. The cylindrical pit also



**Figure 3** Variation of cylindrical pit interior mean temperature over a lunar day with latitude.

achieves the lowest nighttime mean temperatures because most facets within the pit “see” a larger sky fraction than most facets within the other geometries and are therefore able to more efficiently radiate energy away to space.

**Conclusions:** Efficient shadowing means that the interior temperatures of the modeled pits and attached caves are strongly controlled by multiple-scattering of infrared radiation. Steep walls and enclosures cause increased facet-to-facet radiative heating because much of the energy that facets would otherwise radiate away to space is directed back towards other parts of the pit/cave. The combination of shadowing and efficient multiple-scattering leads to more enclosed features having more stable temperatures (Fig. 4).

The mean temperatures of the modeled pit/cave geometries mostly remained above 110 K (Fig. 4), which is commonly used as a cut-off temperature above which water ice is not stable on billion-year timescales [2]. This suggests that these features may not form effective cold-traps for  $\text{H}_2\text{O}$ . However, the geometry of these features could still slow volatile escape and limit solar UV photodestruction of volatile molecules. (e.g., a large cave system with a small opening to the surface). The next step in this work will be to apply the volatile transport model to the thermal model output and thus incorporate the effects of both temperature and geometry. While the thermal environments within high-latitude pits/caves may not make them ideal cold-traps, they could provide warmer, more thermally stable environments from which to explore large cold-traps that exist within polar craters.

**References:** [1] Wagner R. V. and Robinson M. S. (2014) *Icarus*, 237, 52-60. [2] Watson K. et al. (1961) *JGR*, 66, 1598. [3] Lee P. (2018) *LPSC 49* Abstract #2083. [4] Avent W. and Lee P. (2021) *LPSC 52*, Abstract #2548. [5] Hooper, D. M. et al. (2021) *LSSW XII*, Abstract #8025.